



# Fibrinogen-Related Protein, Fgl2, of Hamster Cauda Epididymal Fluid: Enzymatic Characterization, and Identification of Fgl2-Binding Proteins and Ligand of Defective Hamster Sperm Organelles

Nagdas SK<sup>1\*</sup>, Britney T<sup>1</sup>, Simpson D<sup>1</sup>, Salters T<sup>1</sup> and Raychoudhury SS<sup>2</sup>

<sup>1</sup>Department of Chemistry, Physics & Materials Science, Fayetteville State University, USA

<sup>2</sup>Department of Biology, Chemistry and Environmental Health Science, Benedict College, USA

\*Corresponding author: Subir K Nagdas, Department of Chemistry, Physics & Materials Science, Fayetteville State University, USA, Tel: 910-672-2073; Email: snagdas@uncfsu.edu

Research Article

Volume 8 Issue 2

Received Date: August 24, 2023

Published Date: September 26, 2023

DOI: 10.23880/ijbp-16000228

## Abstract

The luminal environment of the mammalian epididymidis performs a dual function; sperm maturation and maintaining sperm viability. We previously identified a secretory protein (260/280KDa oligomers) of hamster cauda epididymal principal cells that binds to nonviable sperm. The 260/280KDa oligomers are composed of 64kDa FGL2 (fibrinogen-like protein-2) and 33kDa FGL1 (fibrinogen-like protein-1). The potential mechanism by which FGL2 binds to degenerative sperm is not clearly demonstrated. In this study, we report the downstream sequence of prothrombinase activity of FGL2, the identification of organelles, and characterize candidate proteins that bind FGL2. The following reaction sequence confirms that FGL2 is a phospholipid-activated serine protease; the conversion of prothrombin to thrombin by FGL2, followed by the conversion of soluble fibrinogen to insoluble fibrin polymers by thrombin. FGL2 binds intensely to tails than heads of de-membrated sperm. A spectrum of polypeptides of cauda sperm tails binds to FGL2. Proteomic analyses of 65KDa, 16kDa, and 13kDa polypeptides of tails correspond to a-Kinase anchor protein 4, glutathione peroxidase 4, and cytochrome c oxidase subunit 4, respectively. Annexin V, a calcium-dependent phosphatidylserine-binding protein localized to the flagellum and co-precipitated with FGL2. We have demonstrated a novel protective mechanism for recognizing and eliminating defective spermatozoa from viable sperm population.

**Keywords:** Hamster Sperm-Epididymis- Fibrinogen-Like Protein-2 (FGL2); Prothrombinase-Annexin V

**Abbreviations:** ELSPBP1: Epididymal Sperm Binding Protein 1; FGL2: Fibrinogen-Like Protein-2; DCF: Death Cocoon Fraction; NCBI: National Center For Biotechnology Information; CEF: Cauda Epididymal Fluid.

## Introduction

Mammalian spermatozoa exiting the testis are functionally immature and require a series of post-testicular morphological and biochemical modifications in

the epididymis to achieve forward motility and fertilizing capacity [1,2]. During the transit through the epididymis [3,4], spermatozoa experience a continuously modulated luminal fluid environment of region-specific ionic, organic solute, and protein composition [2,5,6]. Sperm maturation and storage functions of the epididymis depend upon paracrine interactions between the epididymal epithelium and spermatozoa [5,7]. The luminal environment is regulated by the secretory and absorptive activities of the epididymal epithelium, which in turn is controlled by androgens and

testis-derived factors [5,6]. The luminal environment of the epididymis has a dual function. In the proximal epididymis, it promotes sperm maturation, and in the distal cauda epididymis, it maintains sperm viability during storage [1,7-12]. The epididymal epithelium secretes enzymes involved in glutathione conjugation and metabolism [7,13] that are thought to prevent oxidative damage to the sperm plasma membrane, sulfated glycoprotein-2 (SGP-2 or clusterin) that is proposed to inhibit complement-mediated cell lysis, and potential protease inhibitors such as HE4 [14] and CRES [15] that may protect spermatozoa from proteolytic degradation. Although several studies proposed the putative roles of epididymal secretory proteins, the precise function of epididymal secretory proteins in sperm maturation and survival is not clearly understood. The presence of dead spermatozoa in the cauda epididymis region has been observed in many species; not all spermatozoa remain viable during passage through the epididymis; [16-18]. In the hamster, the nonviable sperm population increases along the length of the epididymis [18]. In several species, aggregated masses of degenerating spermatozoa that are embedded in an amorphous electron-dense material have been noted within the lumen of the cauda epididymidis and vas deferens [17,19]. Olson, et al. [20] proposed that degenerating spermatozoa release enzymes that may compromise the viability of neighbouring cells. Alternatively, these released enzymes/antigens may be a source of autoantigens that could induce the immune response if they escape the blood-epididymis barrier. Anti-sperm antibodies are not uncommon in men. They develop for reasons that are not understood, and they are a source of infertility that is difficult to correct [21,22]. It is critical to determine if the epididymis plays a significant role in preventing these adverse effects on male fertility.

What are the protective strategies of the epididymis that could prevent these negative impacts on male fertility? It is not clearly resolved whether degenerating spermatozoa undergo death by an apoptotic pathway [23]. Some investigators have suggested that human spermatozoa exhibit apoptosis [24,25]. It has been reported that sperm death appears to be caspase-independent [26]. The nuclear tumor suppressor protein, p53, and the cell surface protein, Fas, a tumor necrosis factor family member, are not associated with sperm death in the epididymis [27,28]. There is no evidence of significant sperm phagocytosis by the normal epididymal epithelium *in vivo* [3,29]. Since dead spermatozoa appear to remain in the epididymal lumen until eliminated in the ejaculate [30,31], it seems critical to define the mechanisms which physiologically separate the dead and viable sperm populations. Whether specific changes on the sperm surface signal the onset of its death is an important unresolved question. Spermatozoa, subjected to oxidative stress or cryopreservation, possess increased

annexin V binding—an indication of membrane changes due to externalization of phosphatidylserine (PS) [32-36]. Annexin V also binds products of lipid peroxidation [37-39]. The sperm plasma membrane is illustrious by a high content of polyunsaturated fatty acids [40-43], which renders it a target for the deleterious effects of lipid peroxidation induced by reactive oxygen species [44,45]. The surface ubiquitination of defective epididymal spermatozoa was demonstrated in several mammalian species and was suggested to target defective spermatozoa for phagocytotic elimination by the epididymal epithelium [46-48]. Other investigators disagree with the proposed sperm elimination mechanism [49]. D'Amours, et al. [50] identified and characterized epididymal sperm binding protein 1 (ELSPBP1) secreted from the principal cells of the epididymis which transfer to bovine dead spermatozoa by epididymosomes in the presence of zinc and proposed that only dead spermatozoa are receptive to ELSPBP1.

Nagdas, et al. [51] proposed another mechanism for recognizing and masking of abnormal spermatozoa. Previously, we identified a hamster epididymal secretory protein of 64kDa (originally termed HEP64). Both luminal fluid and sperm-associated HEP64 are assembled into disulfide-linked oligomers of ~260kDa and ~280kDa. HEP64 is secreted by the principal cells of cauda epididymidis, and it binds explicitly to nonviable sperm and then polymerizes into a proteinaceous “death cocoon” that coats defective spermatozoa and sperm fragments [51]. HEP64 was cloned by expression screening of a hamster cauda epididymal cDNA library and identified as the hamster fibrinogen-like protein 2 (fgl2) [20], a fibrinogen-related family member containing a C-terminus fibrinogen-like domain [52] and an orthologue of mouse and human fgl2 [53-55]. Our biochemical characterization, proteomic analyses, and molecular studies revealed that the high molecular weight oligomer (260/280kDa; termed as eFGL) is composed of two subunits: a 64kDa polypeptide identified as fibrinogen-like protein-2 (FGL2) [20], and a 33kDa polypeptide identified as fibrinogen-like protein-1 (FGL1) [56]. The 33kDa subunit has been fully sequenced and represents the hamster orthologue of a second fibrinogen-related protein termed FGL1 [56]. Several studies proposed that FGL1 plays an important role in biological functions other than coagulation [57-62]. Our data represent the first demonstration of FGL1 protein expression and its functional interaction with FGL2 [56]. Northern blot analysis and *in situ* hybridization studies of hamster tissues demonstrate very high FGL2 [20] and FGL1 mRNA [56] expression in the principal cells of the proximal cauda epididymidis and only limited expression in other tissues. Thus, we have identified two highly expressed and secreted fibrinogen-related proteins produced by the hamster cauda epididymidis. Our previous studies reveal that FGL2 and FGL1 proteins specifically bind defective

spermatozoa and sperm fragments and then polymerize into a “death cocoon,” segregating the defective sperm from the viable sperm populations [20,51,52]. Recently, we purified FGL2 from hamster cauda epididymal fluid towards homogeneity, and its prothrombinase catalytic activity was examined [63]. Time-course conversion studies revealed that all prothrombin was converted to thrombin by purified hamster FGL2 [63]. Our biochemical studies demonstrate that FGL2 is a lipid-activated serine protease and functions as a lectin by binding specific carbohydrate residues. Co-immunoprecipitation analysis demonstrated that FGL2 of cauda epididymal fluid is ubiquitinated but not FGL1 [63].

Several critical questions regarding the mechanism of action of FGL2 remain to be resolved. The objectives of the present study are to examine the downstream sequence of catalytic activity of FGL2. Then, we initiate our studies to identify whether FGL2 binds distinct organelles of intact and de-membranated cauda epididymal spermatozoa and to identify FGL2 binding proteins of sperm organelle. In addition, we also determine if phosphatidylserine (PS) represents surface markers of defective spermatozoa that bind FGL2.

## Materials and Methods

### Animals

Mature male golden hamsters were housed in Benedict College (Columbia, SC). Animal Care Facility on a 14L: 10D cycle and given free access to food and water. Care and use of animals conformed to NIH guidelines for humane animal care and use in research. All protocols were approved by the Institutional Animal Care and Use Committee and the University veterinarians who supervised animal care. Animals were sacrificed by CO<sub>2</sub> asphyxiation, and tissues were immediately removed for the protocols described below.

### Preparation of Epididymal Sperm and Luminal Fluid Samples

The cauda epididymides were dissected and minced in calcium-free Tyrode solution at 37°C. The sperm suspension was centrifuged at 100 × g for 1 min to sediment tissue fragments, and the supernatant fluid was recentrifuged at 1,500 × g for 10 min at 4°C. Sperm pellets were used in the extraction and fractionation protocols described below, while the supernatant fluids, representing crude cauda epididymal luminal fluids, were centrifuged at 100,000 × g for 20 min in a Beckman TL55 rotor (NagDas, et al. 2000). The supernatants were collected and used for the following experiments.

**Isolation of Sperm Heads and Tails:** The published procedure of Nagdas, et al. [64] was followed to isolate the heads, tails, and cytosol from hamster cauda epididymal spermatozoa. The washed sperm pellet was resuspended into 35 ml of TNI [150 mM NaCl, 25 mM Tris-HCl (pH 7.5), 2 mM benzamidine, 1 µg/ml leupeptin, 1 µg/ml pepstatin, and 0.05% sodium azide] and sonicated for 10-sec intervals four times with a Branson sonifier (Branson Ultrasonic Corp., Danbury, CT) at a medium power setting. The samples were examined by phase contrast microscopy to ensure that > 90% of the sperm were decapitated. The sonicated suspension was centrifuged at 1500 g for 10 min. The supernatant was used to prepare cytosol by centrifugation at 100,000 × g for 30 min in a Beckman TL55 rotor, while the sperm pellet was washed three times by resuspension in TNI followed by centrifugation at 1500 X g for 10 min. The final pellet was resuspended with 60 ml TNI, and 10-ml aliquots were layered on discontinuous sucrose gradients composed of 10 ml 55% sucrose, 5 ml 70% sucrose, and 5 ml 75% sucrose; all sucrose solutions contained 25 mM Tris-HCl, pH 7.5. The gradients were centrifuged at 25, 000 rpm for 60 min in a Beckman SW28 rotor (Beckman Instruments, Palo Alto, CA). Tails banded at the 55%/70% interface, and the heads were present in the pellet. Head and tail fractions were collected, diluted with TNI, and pelleted by centrifugation at 1500 X g for 10 min. Phase contrast microscopy examination showed the homogeneous preparation of tails whereas heads were contaminated by few tails.

### Isolation of Death Cocoon Fraction (DCF)

Hamster cauda sperm death cocoon fractions were isolated following the method of Olson, et al. [20]. Briefly, sperm suspensions were prepared by mincing freshly dissected cauda epididymides in calcium-free Tyrode's solution containing 0.5 mM EGTA and 2 mM benzamidine. Aliquots of the sperm suspension (6 ml) were layered over an isotonic discontinuous Percoll gradient composed of 2 ml of 20% Percoll and 2 ml of 40% Percoll in Tyrode's solution. The gradients were centrifuged at 1,500 × g for 10 min. The particulate fraction that layered on top of the 20% Percoll was collected, diluted with ice-cold Tyrode's solution, and then sedimented at 100,000 × g for 60 min in a Beckman SW41 rotor. The isolated DCF fraction was suspended in TNI for the following biochemical analyses.

### Gel Electrophoresis and Western Blotting

Polypeptides were separated by SDS-PAGE [65] on a 12% separation gel prepared with a 30:0.8 acrylamide:bisacrylamide ratio. Polypeptides were stained with Coomassie Brilliant Blue (CBB) [66]. Western blots were prepared on polyvinylidene difluoride membranes for

immunoblot analysis [67]. Proteins were estimated by the method of Bradford [68].

Immunoblots were blocked with TBS (0.15 M NaCl, 20 mM Tris-HCl Buffer, pH 7.5) containing 0.1% Tween 20 and 1% BSA and then incubated with immune serum (rabbit polyclonal anti-FGL2/ rabbit monoclonal fibrinogen beta chain [abcam] /mouse monoclonal Annexin V/ ANXA5 [abcam] antibodies) or nonimmune serum diluted in TBS containing 0.1% Tween 20 (TBS-TW) and 1% BSA. After three washes in TBS-TW, the blots were incubated in an affinity-purified, peroxidase-conjugated goat anti-rabbit or anti-mouse IgG secondary antibody (KPL Inc., Gaithersburg, MD) diluted in TBS-TW. For LICOR Odyssey CLx Imaging System IRDye® 680RD, goat anti-mouse and goat anti-rabbit diluted in TBS-TW were used. Following several TBS-TW washes, immunoreactive bands were identified either by LICOR Odyssey CLx Imaging System or by chemiluminescence using SuperSignal (Pierce) and detection on Kodak BioMax film or by color development using  $H_2O_2$  and diaminobenzidine.

### Purification of FGL2 from Hamster Cauda Epididymal Fluid

The homogeneous fraction of FGL2 was purified from hamster cauda epididymal fluid following the method of Nagdas, et al. [63]. The Siliconized glass columns were used for chromatography, and all procedures were performed at 4°C. The homogeneous FGL2 fraction was conjugated with NHS-LC-biotin (Pierce Chemical Co., Rockford, IL) following the manufacturer's protocol. The efficacy of FGL2 biotinylation was examined by incubation in peroxidase-avidin (Vectastain ABC Kit, Vector laboratories, Burlingame, CA), followed by color development with diaminobenzidine and  $H_2O_2$ .

### Immunofluorescence Microscopy

Sperm suspension of cauda epididymis was fixed for 15–30 min at 4°C with 4% formaldehyde, 0.1 M sodium phosphate buffer, pH 7.4 (PBS) and plated on poly-L-lysine-coated coverslips. After three rinses in PBS containing 0.05% Tween 20, nonspecific protein binding sites were blocked in PBS containing 1% normal goat serum, 1% normal donkey serum, and 2.5% BSA. After three rinses in PBS containing 1% normal goat serum (PBS-NGS), coverslips were incubated with equal dilutions of immune or nonimmune serum in PBS-NGS for 1 hr. and washed three times with PBS-NGS. Cells were then incubated with Cy3-conjugated goat anti-rabbit IgG or FITC-conjugated goat anti-mouse IgG (KPL Inc., Gaithersburg, MD) in PBS-NGS for 1 hr. Coverslips were washed with PBS and were examined by phase contrast and epifluorescence microscopy.

### Enzymatic Assay of FGL2

Recently, we had shown that homogeneous fraction of Fibrinogen-like protein-2 (FGL2) of hamster cauda epididymal fluid is a phospholipid-activated serine protease that cleaves prothrombin to thrombin in in vitro assays [63]. The current study examined the downstream sequence of FGL2 catalytic activity. The homogeneous fraction of FGL2 was purified following the procedure of Nagdas, et al. [63]. Fibrinogen, prothrombin, and fibrin were purchased from Sigma-Aldrich Chemical Company. First, the conversion of prothrombin to thrombin by purified FGL2 was performed by incubating 20µg prothrombin and 0.12µg of FGL2 in a 50µL solution containing 50mM Tris-HCl (pH 8), 100mM NaCl, and 5mM  $CaCl_2$  at 37°C for 12 hrs. Then, fibrinogen (0.2mg) was added to the reaction mixture after converting prothrombin to thrombin by FGL2 and incubated for 6 hrs. at 37°C followed by centrifugation at 40,000rpm for 30 mins. The supernatant was collected, and the pellet was washed in TNI [150 mM NaCl, 25 mM Tris-HCl (pH 7.5), 2 mM benzamidine, 1 µg/ml leupeptin, 1 µg/ml pepstatin, and 0.05% sodium azide] one time by centrifugation at 40,000rpm for 30 mins. Finally, washed pellet was suspended in a volume of TNI equal to the volume of supernatant. As a control, parallel reaction was performed without the addition of fibrinogen where no precipitation was found. Both supernatant and pellet fractions of experiment and control were analyzed by Western Blot analysis stained with rabbit monoclonal antibody to fibrinogen β chain. Immunoreactive bands were visualized by color development with diaminobenzidine and  $H_2O_2$ .

### To identify which organelles of defective spermatozoa, bind FGL2

This experiment was performed to determine whether FGL2 binds to distinct organelles of intact and de-membranated cauda epididymal spermatozoa. De-membranated spermatozoa were prepared using nitrogen cavitation at 400 psi since this treatment partially removes the plasma membrane but did not release intracellular membranes or organelles [69]. Suspensions of intact and de-membranated spermatozoa (~106 sperm/ml) were incubated with the biotinylated-FGL2 (10ug/ml) for 1 hr. Sperm were gently washed and then incubated in Streptavidin-Alexa Fluor™ 594 conjugate (Invitrogen) for 1 hr., followed by final PBS washes to remove nonbounded probes. Alexa 594-avidin-labeled spermatozoa were examined by fluorescence microscopy. Previously, we had shown FGL2 functions as a lectin by binding specific carbohydrate residues using neoglycoproteins consisting of BSA conjugated to specific carbohydrates [63]. The binding affinities of galactose and glucose neoglycoproteins were

greater than other neoglycoproteins [63]. In the present study, to examine the specificity of FGL2 binding to intact and de-membrated spermatozoa, the mixture of glucose and galactose (0.2M each) were used as competitors to block FGL2 binding to spermatozoa.

### Binding of Biotinylated FGL2 to Heads, Tails and Cytosol

The binding of biotinylated FGL2 to organelles was performed utilizing a dot blot assay. The heads and tails were extracted in RIPA buffer (1% Triton X-100, 1% sodium deoxycholate, 0.1% SDS, 0.15 M NaCl, proteases inhibitors in 10 mM sodium phosphate buffer, pH 7.2) for 2 hrs at 4°C and then centrifuged at 40,000 rpm for 30 min in a TL55 rotor (Beckman). The supernatant (RIPA-Supernatant) was collected, and the protein was estimated BCA protein assay Kit (Pierce Chemical Co., Rockford, IL) following the manufacturer's protocol. The aliquots of known protein concentrations were spotted on nitrocellulose membranes. Membranes were blocked in PBS containing 5% BSA and then incubated in a blocking solution containing biotinylated FGL2. After several washing in PBS, the blots were incubated in peroxidase-avidin (Vectastain ABC Kit, Vector laboratories, Burlingame, CA) for detection by color development with diaminobenzidine and H<sub>2</sub>O<sub>2</sub>.

### Blot Overlay Assay

A blot overlay assay was employed to identify FGL2-binding polypeptides of the hamster sperm tails [70]. Isolated sperm tails were separated by SDS-PAGE [65] and transferred to PVDF membranes [67]. Blots were washed three times for 30 min each at 40°C with binding buffer composed of 25 mM Tris-HCl (pH 7.0) and 50 mM NaCl and then incubated in 1% BSA in binding buffer. The blot was then incubated overnight at 40°C in a binding buffer containing biotinylated FGL2 (10µg/ml). The blot was then rinsed two times with a binding buffer and once with 20 mM Hepes, pH 7.4, and then fixed with 1% glutaraldehyde in 20 mM Hepes, pH 7.4, for 15 min at room temperature. The blot was then washed with binding buffer and treated for 15 min with binding buffer containing 0.1 M glycine to block free aldehyde residues. FGL2 binding proteins were identified by incubation in peroxidase-avidin (Vectastain ABC Kit, Vector laboratories, Burlingame, CA), followed by color development with diaminobenzidine and H<sub>2</sub>O<sub>2</sub>.

### Proteomic Analysis

Proteomic identification of three major FGL2 binding polypeptides of hamster sperm tails by LC-MS/MS on the Orbitrap Elite mass spectrometers was performed at the

Mass Spectrometry Facility of the Medical University of South Carolina, Charleston, SC. Three CBB stained bands were excised from SDS-PAGE gel, were subjected to trypsin digestion, peptide extraction, and desalting followed by LC-MS/MS analysis. Derived peptide sequences were analyzed in the National Center for Biotechnology Information (NCBI) database to determine potential functional motifs, including a transmembrane hydrophobic domain, an extracellular domain with consensus glycosylation sites, and to define potential phosphorylation sites and protein interaction domains on its cytoplasmic segment.

### Immunoprecipitation

Cauda epididymal sperm were extracted in TNI having 0.1% Triton X-100 for 2 hours at 4°C and then centrifuged at 40,000 rpm for 30 min in a TL55 rotor (Beckman). The supernatant was collected and was precleared of endogenous IgG by incubation with Protein A Sepharose beads for 15 min at 4°C and centrifugation at 12,000 X g for 1-2 min. The supernatant (50µg protein), free of endogenous IgG, was immunoprecipitated with anti-FGL2 using Pierce™ Crosslink Magnetic IP/Co-IP Kit (Pierce Chemical Co., Rockford, IL) following the manufacturer's protocol. Control immunoprecipitations utilized nonimmune IgG conjugated to Protein A-Sepharose 4B. The beads containing bound proteins were washed two or three times by centrifugation in TNI. The bound protein was then eluted with 0.1M Glycine-HCl buffer, pH 2.5, and neutralized to pH 7.0. Immunoprecipitated proteins in acid-eluted fractions were fractionated by SDS-PAGE, transferred to PVDF membranes, and stained with anti-FGL2 and anti-annexin antibodies.

## Results

### Enzymatic Properties of FGL2

Our previous study reveals that FGL2 is a phospholipid-activated serine protease and converts prothrombin to thrombin [63]. In the current study, we examine the conversion of soluble fibrinogen to insoluble fibrin polymers by thrombin produced by FGL2 from prothrombin. After the completion of the reaction, the supernatant and the pellet fractions were analyzed by immunoblot analysis (Figure 1). The supernatant (lane 1), pellet (lane 2) fractions, and fibrin protein as a positive control (lane 5) demonstrated the presence of an immunoreactive 56kDa fibrinogen β chain band and other bands. No band was detected when identical lanes of supernatant (lane 3) and pellet (lane 4) were stained with nonimmune serum. A significant portion of the 56kDa fibrinogen β was present in the pellet (lane 2), demonstrating the conversion of soluble fibrinogen to insoluble fibrin polymers. Other immunoreactive bands

could be different fibrin polymers having different molecular weights. The current study and our previous results strongly confirm that FGL2 of hamster cauda epididymal fluid (CEF) is a phospholipid-activated serine protease.

### To identify which Organelles of Defective Spermatozoa, Bind FGL2

The biotinylated FGL2 (Figure 2-I) was used to determine whether FGL2 binds distinct organelles of intact and de-membranated cauda epididymal sperm. Previously Nagdas et al. [51] and Olson et al. [20] demonstrated that FGL2 binds only defective spermatozoa (quantitatively 9-13% of the total sperm population), not the morphologically normal cauda epididymal spermatozoa. In the current study, we have also shown a discrete localization pattern of cauda epididymal spermatozoa immunostained with anti-fgl2. Most cauda epididymal spermatozoa exhibited no fluorescence staining (Figure 2-II-A), and companion phase-contrast images (Figure 2-II-A') demonstrated that the unstained spermatozoa appeared morphologically normal. Surprisingly, one spermatozoan (Figure 2-II-A) shows that the acrosome was misshapen or absent and a degenerating sperm tail stained intensely with anti-fgl2. In the present study, we also counted at least two hundred spermatozoa from the cauda epididymides of three animals and we confirmed our previous quantitative observation which is 9-13% of the total sperm population stained with anti-fgl2. All our studies strongly demonstrate that FGL2 selectively associates with damaged spermatozoa.

De-membranated spermatozoa were prepared using nitrogen cavitation at 400 psi since this treatment results in partial removal of the plasma membrane but do not release intracellular membranes or organelles [69]. Suspensions of de-membranated spermatozoa (~106 sperm/ml) were incubated with the biotinylated-FGL2 (10 ug/ml) for one hr. The spermatozoa were gently washed and then incubated in Alexa 594-avidin for one hr., followed by final PBS washes to remove non-bound probes. Alexa 594-avidin-labeled spermatozoa were examined by fluorescence microscopy. Our results showed that the tails and heads bind biotinylated FGL2; however, more intense binding was observed in tails than in the heads of de-membranated spermatozoa (Figure 2-II-B). By dot blot assay, we had shown that biotinylated FGL2 binds specific carbohydrate residues in a dose dependent manner and the binding affinities of galactose and glucose were greater than other carbohydrates [63]. Our current cytochemical studies revealed that no binding of biotinylated FGL2 (Figure 2-II-C) was observed when de-membranated sperm were incubated in glucose and galactose (0.2M each),

confirming the specificity of biotinylated FGL2 binding to the de-membranated sperm population. This study confirms that the tails of de-membranated spermatozoa bind strongly to FGL2.

### Binding of FGL2 to Heads, Tails and Cytosol

Cytochemical studies revealed that heads and tails of de-membranated spermatozoa bind to FGL2, although a strong binding affinity was observed in tails (Figure 2-II-B). Next, we examined the binding affinity of biotinylated FGL2 to heads, tails, and cytosol by dot blot assay. The binding affinity of biotinylated FGL2 (Figure 3A) was greater in tails (Row#3) than in heads (Row#1); no binding was noted in the cytosol (Row#2). Our data showed the binding specificity of biotinylated FGL2 to tails. Since a strong binding affinity was observed between tails and FGL2, our subsequent study was initiated to identify and characterize tail polypeptides that specifically bind FGL2.

Identification and Characterization of FGL2 Binding Proteins in Tails: To identify candidate proteins of tails that are associated with FGL2, tails (25 µg proteins) were subjected to blot overlay assay probing with biotinylated FGL2 (Figure 3B, lane 3). An identical lane (Figure 3B, lane 2) was stained with CBB. Three distinct polypeptides (65kDa, 16kDa, and 13kDa) of sperm tail polypeptides bind to FGL2 among the spectrum of polypeptides (lane 3), and the companion CBB stained (lane 2) also exhibit three corresponding polypeptides. Next, we performed the proteomic identification of three individual polypeptides by LC-MS/MS analysis. Proteomic data are shown in Table 1. Band 1 (65kDa) yielded twenty-nine peptides matching A-kinase anchor protein 4 (*Mesocricetus auratus*; accession: A0A1U7RDU8), band 2 (16kDa) generated eleven peptides matching glutathione peroxidase (*Mesocricetus auratus*; accession: A0A1U7QXX6), and band 3 (13kDa) yielded eleven peptides matching cytochrome c oxidase subunit 4 (*Mesocricetus auratus*; accession: A0A1U8BYF8). These experiments demonstrate a significant interaction exhibited between tail proteins and FGL2.

It is also possible that FGL2 plays key, protective functions by binding specific ligands expressed on defective spermatozoa and the potential ligand could be the externalized phosphatidylserine (PS). In normal cells, PS localizes on the inner plasma membrane leaflet. Our next study was initiated to characterize Annexin V, a calcium-dependent PS-binding protein of hamster cauda epididymal spermatozoa.

Bands from Lane 2	Protein	Matches Peptides
Band 1 (65kDa)	<b>A-Kinase Anchor Protein 4</b> (Mesocricetus auratus)	NLHNITGVLMTDSDFVSAVKR LVSALLGEKKETK ERQLDEAVGNmAKK LLESEPFScDDLPEGENKR YSNNGAALAELEEQAAMAGGSSR ERQLDEAVGNmAK GKDIcEDEcPGSSmGYmSQSTQYEK cLHHSIYASPGEK SVATSDAEcSmDDLsfyVNR KTFlySELSNK RLVSALLGEK RPEDQcPDSSEQDFISGmKQmNR DSKEFADSISK IASEmAHEAVELTSAEmR AAEKGYSGDLLQEVmK TFLYSELSNKNK SQSLAYATLK QFIDQLVESVmK QNAADImEAmLKR SLSmKHFESR LVSALLGEK NTNNNQSPSNPAAK LSPSTDSLAK NQSLEFSAmK QLDEAVGNmAK QLDEAVGNmAKK TFLYSELSNK LSSLVIQmAR LDmSNmVLSLIQK
Band 2 (16kDa)	<b>Glutathione Peroxidase 4 (GpX4)</b> (Mesocricetus auratus)	TDVNYTQLVDLHAR QEPGSNQEIKEFAAGYDVK QEPGSNQEIK RYGPmEEPLVIEK YGPmEEPLVIEK GRGmLGNAIK FLIDKNGcVmKR SmHEFSAK ILAFPcNQFGKQEPGSNQEIK GmLGNAIK FDmYSK
Band 3 (13kDa)	<b>Cytochrome C Oxidase subunit 4</b> (Mesocricetus auratus)	mLDmKANPIQGFSK EKADWSSLSRDEK ADWSSLSRDEK RDYPLPDVAHVK AHGSVVKSEDYALPmYmDR

**Table 1:** Identification of FGL2 Associated Proteins by LC-MS/MS Proteomic Analysis.

### Immunoblot and Immunofluorescence of Annexin V

Immunoblot analysis of cauda epididymal sperm (lane 1) and death cocoon fraction (lane 2) stained with anti-

Annexin V revealed the presence of a 36.8kDa Annexin V band (Figure 4-I). The antibody of Annexin V was utilized to localize Annexin V on the surface of abnormal spermatozoa. Immunofluorescence (Figure 4-II A) and matched phase contrast (Figure 4-II A') images of intact hamster cauda

epididymal spermatozoa stained with anti-Annexin V, revealed that the flagellum of defective spermatozoa, not the morphologically normal sperm population stained with anti-Annexin V. Specifically, two defective spermatozoa tail, shown by arrow (Figure 4-II A) stained intensely with anti-Annexin V and companion phase-contrast image, shown by arrow (Figure 4-II A') demonstrated that those two sperm appeared morphologically abnormal, and unstained spermatozoa appeared morphologically normal. Sperm stained with nonimmune serum exhibited no fluorescence.

Nitrogen cavitated de-membrated spermatozoa revealed the intense staining of flagellum with anti-Annexin V; no staining was evident in heads (Figure 5A), and matched phase contrast (Figure 5A') image revealed a dense population of detached heads and tails. Surprisingly, nitrogen-cavitated de-membrated spermatozoa stained with anti-FGL2 showed intense staining both in detached heads and tails (Figure 5B), whereas no fluorescence was observed in intact spermatozoa as shown by an arrow in companion phase-contrast image (Figure 5B'). Fluorescence micrograph of the tails stained anti-Annexin V (Figure 5C) revealed the intense staining of the flagellum, and companion phase-contrast photomicrograph (Figure 5C') exhibits sperm tails fraction; moreover, few sperm heads exhibited no fluorescence staining. Our indirect immunofluorescence with Annexin V antibody localized Annexin V to the flagellum.

### Co-Immunoprecipitation Studies of Annexin V and FGL2

Co-immunoprecipitation analyses were performed to examine the interaction of FGL2 with Annexin V (Figure 6). Triton X-100-soluble lysates of cauda sperm were immunoprecipitated with anti-FGL2 (Figure 6- A and B). FGL2 (A-lane 1) and Annexin V (B-lane 3) were present in sperm lysate. FGL2 of sperm lysate was recovered in the anti-FGL2 immunoprecipitation (IP) pellet (A-lane 2). Annexin V co-precipitated with FGL2 (IP Pellet-B-lane 4). No immunoreactive bands were observed when an identical blot was stained with nonimmune serum (data not shown). Our co-immunoprecipitation study confirmed the interaction of FGL2 with Annexin V.

### Discussion

Previously, we have shown the prothrombinase activity of hamster cauda epididymal FGL2 converting prothrombin to thrombin and it is a lipid-activated serine protease [63]. Several studies in different tissues have documented the prothrombinase activity of FGL2. [71-74]. It is also reported that coagulation factors (VII, IX, X, XII, and thrombin) have serine protease activity [75-77]. In the present study, further investigation has been conducted to examine the

downstream sequence of the prothrombinase activity of FGL2. We have shown the conversion of soluble fibrinogen to insoluble fibrin polymers (Figure 1, lane 2) by thrombin produced by FGL2 from prothrombin. Both studies strongly demonstrated that FGL2 of hamster cauda epididymal fluid (CEF) is a phospholipid-activated serine protease.

Thus, we have identified two highly expressed and secreted fibrinogen-related proteins (FGL2 and FGL1) secreted by the principal cells of hamster cauda epididymidis which specifically bind defective spermatozoa and sperm fragments and then polymerize into a death cocoon which segregates the defective from the viable sperm populations [20,51,56,63]. Fibrinogen-like protein 2 (Fgl2), a member of the fibrinogen family, can be expressed as a membrane-associated protein with coagulation activity or in a secreted form possessing unique immune suppressive functions. The soluble form of FGL2 is mainly secreted by CD4 + CD25 + Foxp3 + regulatory T cells (Tregs) [78-80] whereas, the insoluble form is a transmembrane protein that integrates with phospholipids of the cellular membrane, which is expressed in endothelial cells, epithelial cells, macrophages, and dendritic cells [73]. The expression of Fgl2 is significantly higher in many cancers, including colon cancer, oesophageal cancer, gastric cancer, breast cancer, lung cancer, skin, and cervical cancer [79-81] where it regulates the proliferation, invasion, and migration of tumor cells, or controls the functions of immune cells in the tumor microenvironment [80]. Fgl2 could be a promising prognostic biomarker, such as early detection of malignancies, tumor progression, allograft rejection, and viral therapy failure. It has been shown that the soluble Fibrinogen-like protein 2 is increased in infertile men with idiopathic causes and with varicocele-induced infertility [82].

Our previous studies [20,51,56,63], along with our current study (Figure 2-II-A) strongly demonstrate that FGL2 binds only the abnormal spermatozoa. It has yet to be determined how FGL2 recognizes and binds defective spermatozoa. Ultrastructural studies reflect that the polymerized death cocoon adheres to membrane vesicles and sperm-specific intracellular organelles, including the acrosome, mitochondrial sheath, outer dense fibers, and fibrous sheath [20,51]. Our current study shows an intense binding of biotinylated FGL2 to the tails of nitrogen-cavitated de-membrated spermatozoa (Figure 2-II-B). We propose that FGL2 has a broad recognition specificity and binds specific residues expressed on the plasma membrane of defective spermatozoa and to specific intracellular organelles of dead spermatozoa, which become exposed by loss or vesiculation of the plasma membrane. Physiologically, this recognition and the binding of FGL2 could justify that sperm autoantigens become immobilized to sperm-specific intracellular organelles or within the death cocoon and are



not available to initiate an autoimmune or inflammatory response.

Our dot blot analysis (Figure 3A) reveals that the affinity of FGL2 binding to tails is greater than heads. Proteomic analysis of 65kDa, 16kDa, and 13kDa polypeptides correspond to a-Kinase anchor protein 4, glutathione peroxidase 4 (GPX4), and cytochrome c oxidase subunit 4, respectively (Table 1). A-Kinase Anchor Protein 4 (AKAP4) is a major component of the sperm fibrous sheath in all mammals so far examined [83-88] and regulates the signal transduction and metabolic pathways that support sperm motility and capacitation [89]. AKAP4 anchors cAMP-dependent protein kinase A (PKA) to the fibrous sheath of the spermatozoon, where the kinase is likely to be required to regulate sperm motility [90,91]. Akap4 knockout animals display aberrant fibrous sheath development, a shortened flagellum, and a substantially reduced abundance of signal transduction and glycolytic enzymes usually associated with the fibrous sheath [92]. AKAP4 plays an important role in the 4HNE (4-hydroxynonenal) induced oxidative stress damage, thus strengthening the importance of AKAP4 as a biomarker of sperm quality [89]. 4HNE (4-hydroxynonenal) is generated during lipid peroxidation [89]. AKAP4 interacts with several other proteins in the fibrous sheath. One of these is AKAP3, another essential component of the fibrous sheath [91,93,94]. In addition, AKAP4 interacts with glutamine-rich protein 2 (QRICH2) [95]. The decreased protein expression of AKAP4 and QRICH2, as well as the interaction between them induced by the hemizygous variant of AKAP4, caused dysplastic fibrous sheath, which eventually led to reduced sperm motility and male infertility [95]. Our current study demonstrates the interaction of FGL2 with AKAP4. It is possible that this interaction of FGL2 to AKAP4 may shield the defective sperm from a healthy sperm population. The mechanism of interaction will be addressed in future studies. GPX4 (also termed PHGPx) is the major disulfide crosslinked sperm mitochondrial protein, and it plays a significant role in forming the mitochondrial capsule [96]. This enzyme also plays an important function in male fertility by affecting the maturation and function of sperm [96,97]. It is believed that male infertility in selenium-deficient animals, characterized by impaired sperm motility and structural abnormalities of sperm tails, is due to insufficient PHGPx content [98,99]. Reactive oxygen species and carbonyl compounds are formed in several physiological pathways. Damaged and immature spermatozoa produced them, are associated with a loss of sperm motility, and have a detrimental effect on sperm-oocyte fusion [41,45,100-102]. The primary cellular enzymatic defense systems against damage from reactive oxygen species are the glutathione redox cycle, the thioredoxin cycle, and catalase [103]. The binding of FGL2 to defective sperm mitochondria may be an additional defense mechanism from reactive oxygen species to protect

the viable sperm population. Cytochrome c oxidase subunit 4 is an important mitochondrial electron transport chain component. In boar spermatozoa, lipopolysaccharide induces mitochondrial oxidative damage [104]. The enzyme activity decreases during spontaneous lipid peroxidation in rabbit epididymal spermatozoa [105]. We propose that the binding of FGL2 to cytochrome c oxidase subunit 4 of defective sperm population will reduce the efficiency of the respiratory chain and gradually promotes their death. This could be a mechanism of elimination of defective spermatozoa. Thus, we have identified three proteins of hamster sperm tails that interact with FGL2. Does this interaction of FGL2 to flagellar proteins play a significant role in segregating the nonviable spermatozoa from the healthy sperm population? Future studies will address this issue. Work is presently in progress to identify and characterize FGL2 binding protein(s) of hamster heads.

We observed that FGL2 binds to the heads and tails of defective spermatozoa, and important functional questions remain to be addressed. What are the specific ligands of defective spermatozoa that bind FGL2? We hypothesize that phosphatidylserine and lipid peroxides expressed on the surface of abnormal spermatozoa represent the physiological membrane ligand for FGL2. Annexin V, calcium-dependent phosphatidylserine (PS)-binding protein, localizes PS. Annexin V is present in hamster cauda sperm (Figure 4-I). Immunofluorescence localization (Figure 4-IIA) of intact hamster cauda epididymal spermatozoa revealed only the tails of defective sperm stained with annexin V antibody; specifically intense staining was present in two defective sperm (shown by arrow) concluding that Annexin V becomes externalized and is exposed on the surface of defective sperm. Our immunofluorescence studies of nitrogen-cavitated demembrated spermatozoa revealed that annexin V was present in the flagellum, whereas anti-FGL2 was stained in detached heads and tails (Figure 5). In addition, co-immunoprecipitation analyses revealed that Annexin V co-precipitated with FGL2 (IP Pellet- Fig.6-lane 4) suggesting that PS may be involved in crosslinking of FGL2 and Annexin V. Whether specific changes on the sperm surface signal the onset of its death is an important unanswered question. Most cells entering the apoptotic pathway coincidentally express PS on the outer leaflet of their plasma membrane [106]. Normally localized to the inner leaflet, PS becomes externalized during apoptosis to be recognized by a common cell surface PS-receptor which triggers phagocytosis of the apoptotic cell [107]. Cell surface PS can be readily identified by its ability to bind the Ca<sup>2+</sup>-dependent PS-binding protein annexin V. Interestingly spermatozoa subjected to oxidative stress, or cryopreservation exhibit increased annexin V binding, a reflection of membrane changes due to externalization of PS [32-36]. PS has been demonstrated on the surface of oxidatively damaged mammalian spermatozoa

[34]. Annexin V also binds products of lipid peroxidation [37-39], and the sperm plasma membrane is distinguished by a high content of polyunsaturated fatty acids [40-42,108], which renders it a target for the deleterious effects of lipid peroxidation induced by reactive oxygen species [44,45]. Despite the elaborate antioxidant systems present in the epididymis, which promote sperm viability [109-111], it is possible that either externalized PS or lipid peroxides are surface markers of the sperm subpopulation destined for death. Do modified sperm plasma membrane lipids serve as receptors of FGL2? It is a critical issue that will be addressed in future studies.

Both the signal that initiates FGL2 binding to abnormal spermatozoa and the mechanisms regulating polymerization of the death cocoon complex remain to be defined. Moreover, phosphatidylserine stimulates the procoagulant activity of macrophage FGL2 [112,113], indicating it could function in binding FGL2 to the cell surface. These observations suggest that phosphatidylserine may represent a recognition signal to initiate FGL2 binding to abnormal spermatozoa and to

promote a protease activity required for the assembly of the sperm death cocoon. It has also been proposed that ubiquitin binds defective spermatozoa by covalent interaction and facilitates the elimination of defective spermatozoa by phagocytosis [47]. With co-immunoprecipitation analyses, we have shown that FGL2 is ubiquitinated but not FGL1 [63]. It could be possible that ubiquitinated surface proteins of defective spermatozoa bind FGL2. Nagdas, et al. [51] demonstrated that the death cocoon complex is also assembled on several sperm-specific structural elements exposed by the loss of the overlying plasma membrane, such as acrosomal components, the post acrosomal sheath, the mitochondrial sheath, and the fibrous sheath. This finding suggests that FGL2 is a pattern recognition molecule that binds one or more common structural motifs in these organelles. Thus, like other fibrinogen-related proteins that function in the innate immune response by recognizing invading pathogens [114-116], FGL2 could recognize newly exposed sperm components via specific exposed domains that may lead to the initiation of death cocoon polymerization.

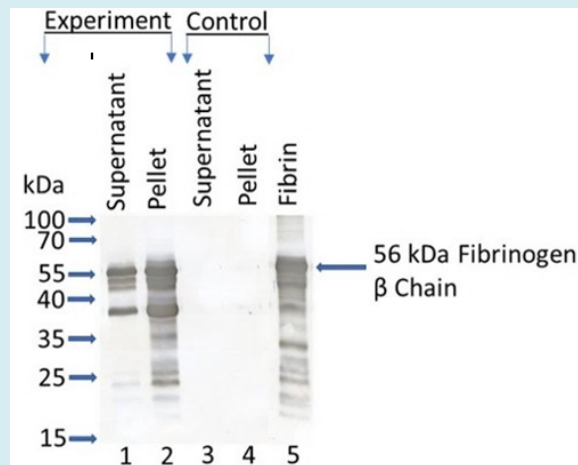


**Figure 1:** Protease Activity of FGL2. Western blot analyses were performed to examine the conversion of soluble fibrinogen to insoluble fibrin polymers by thrombin produced by homogeneous fraction of FGL2 from prothrombin. The homogeneous fraction of FGL2 was purified following the procedure of Nagdas, et al. [63]. Fibrinogen, prothrombin, and fibrin were purchased from Sigma-Aldrich Chemical Company. First, the conversion of prothrombin to thrombin by purified FGL2 was performed. Then, fibrinogen (0.2mg) was added to the reaction mixture after converting prothrombin to thrombin by FGL2. As a control, parallel reaction was performed without the addition of fibrinogen where no precipitation was found. Both supernatant and pellet fractions of experiment and control were analyzed by Western Blot analysis stained with rabbit monoclonal antibody to fibrinogen  $\beta$  chain. Immunoreactive bands were visualized by color development with diaminobenzidine and H<sub>2</sub>O<sub>2</sub>. Note that the 56kDa fibrinogen  $\beta$  was present in the pellet (lane 2) of experiment, demonstrating the conversion of soluble fibrinogen to insoluble fibrin polymers. Other immunoreactive bands in the pellet of experiment (lane 2) could be different fibrin polymers having different molecular weights. Lane 1 represents the supernatant fraction of experiment showing the remaining soluble fibrinogen. Lanes 3 and 4 represent the supernatant and the pellet fractions of control. Lane 5 represents the fibrin (2 $\mu$ g) as a positive control. The results are representative of three experiments.

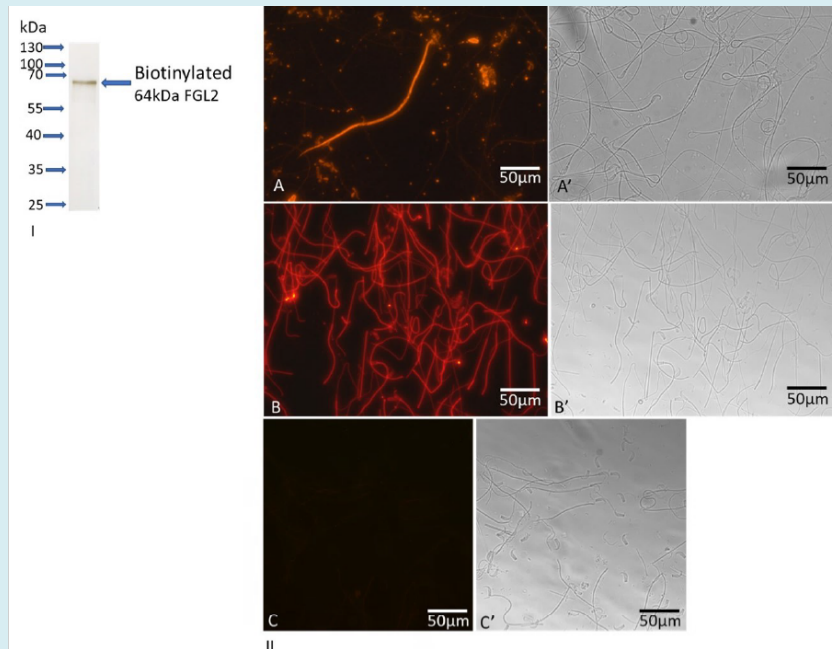


**Figure 2 (I) & (II): Binding of Biotinylated FGL2 to Defective Sperm Organelles. Biotinylated FGL2 (I):** The purified native FGL2 was conjugated with NHS-LC-biotin. Biotinylated FGL2 was used for immunocytochemical studies and dot blot and overlay assays. **Immunocytochemical Studies (II):** Fluorescence (A) and matched phase-contrast (A') photomicrographs of cauda epididymal spermatozoa immunostained with anti-FGL2. Panel A shows a degenerating spermatozoon stained intensely with anti-FGL2, while the intact spermatozoa exhibit no fluorescence. Nitrogen cavitated de-membranated spermatozoa incubated with biotinylated FGL2 followed by Alexa 594-avidin (B) and matched phase-contrast (B') photomicrographs showed that biotinylated FGL2 displays intense fluorescence to tails than heads. To examine the specificity, the binding of biotinylated FGL2 was performed in the presence of glucose and galactose (0.2M each), and no staining was observed either in tails or in heads (C). A companion phase-contrast (C') photomicrograph shows the presence of heads and tails. Bar = 50  $\mu\text{m}$ .

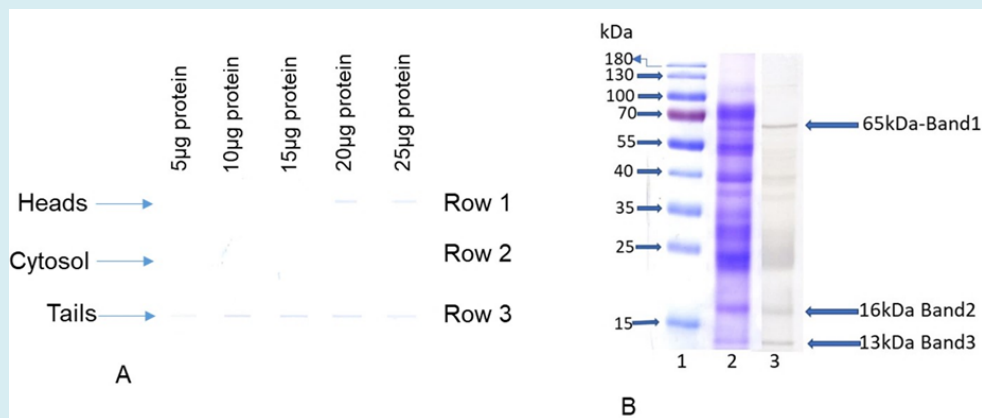


**Figure 3 (A) & (B): Binding of Biotinylated FGL2 to Heads, Tails and Cytosol by Dot Blot Assay (A):** Different concentrations of tails (row #3), cytosol (row #2), and heads (row #1) were examined for the binding efficiency of biotinylated FGL2. The results are representative of three assays. Note that the higher binding affinity is observed in tails (row #3) than in heads (row #1), whereas cytosol shows no binding (row #2). **Blot Overlay Assay of FGL2 binding proteins of tails (B):** Tails were fractionated by SDS-PAGE. Each lane contains 25  $\mu\text{g}$  protein. Lane 2 was stained with CBB, and a companion lane was transferred to the PVDF membrane, followed by a blot-overlay assay probing with biotinylated FGL2 (lane 3). Three distinct polypeptides (65kDa, 16kDa, and 13kDa) of tails bind FGL2 among the several polypeptides (lane 3). Those three bands were excised from the companion CBB-stained gel (lane 2) and subjected to proteomic analyses by LC-MS/MS.

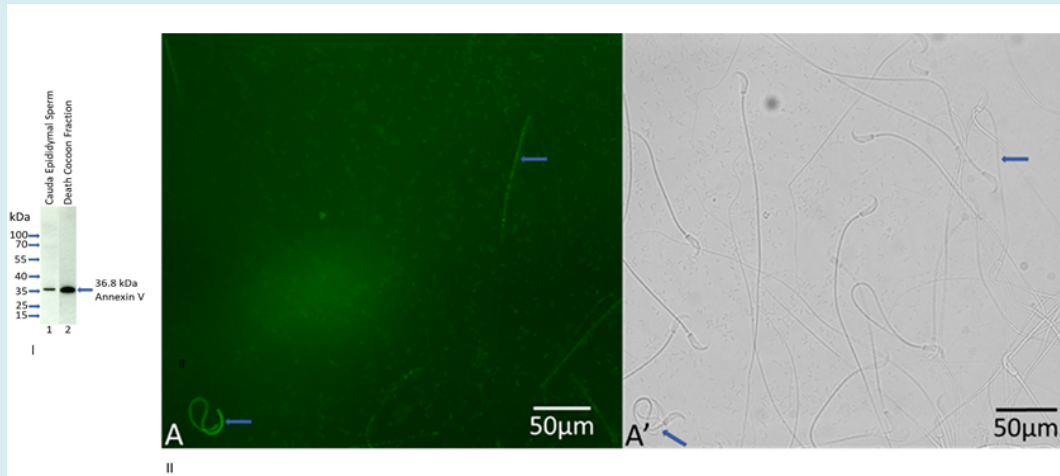


**Figure 4 (I) & (II): Immunoblot of Annexin V (I):** Western blots of cauda epididymal fluid (lane 1) and death cocoon fraction (lane 2) fractionated by SDS-PAGE stained with anti-Annexin V monoclonal antibody. Annexin V immunoreactive band was detected by LICOR Odyssey CVX imaging system. Each lane contains 5 $\mu$ g of protein. **Immunolocalization of Annexin V (II):** Immunofluorescence (Panel A) and a matched phase contrast (Panel A') photomicrographs of intact hamster cauda epididymal spermatozoa immunostained with anti-Annexin V monoclonal antibody. Note that the tails of two defective spermatozoa (as shown by the arrow) are stained with an annexin V antibody (Panel A).

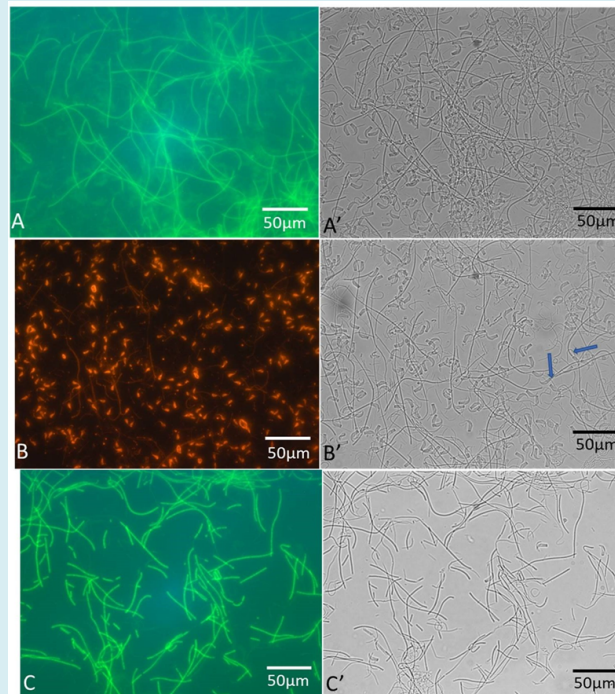


**Figure 5: Immunolocalization of Annexin V and FGL2 in isolated heads and tails.** Panel A shows the localization of Annexin V in the flagellum of nitrogen-cavitated cauda sperm; no staining was observed in heads. A matched phase contrast micrograph (Panel A') reveals the presence of detached heads and tails. Panel B reveals the presence of FGL2 in detached heads and tails of nitrogen-cavitated cauda sperm when immunostained with anti-FGL2; no staining was evident in intact spermatozoa (as shown by arrow) in a companion phase contrast micrograph (Panel B'). Panel C shows a fluorescence micrograph of isolated tails stained with anti-Annexin V. An intense staining was evident in the flagellum, and no fluorescence was observed on heads (Panel C). Few sperm heads are present in isolated tails, as shown in the companion phase contrast micrograph (Panel C'). Bar = 50  $\mu$ m.

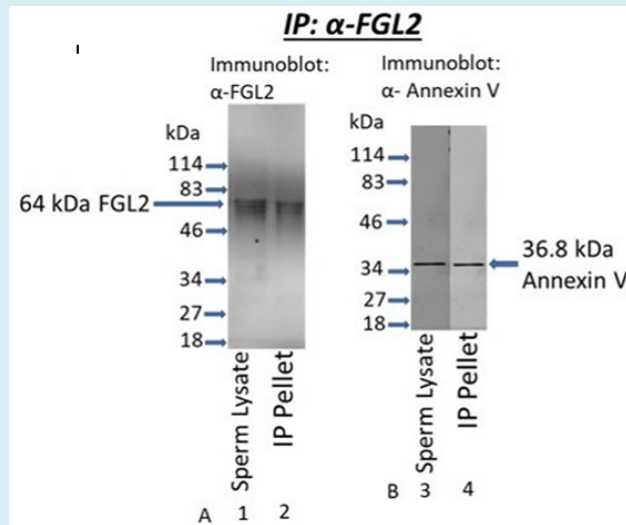


**Figure 6: Coimmunoprecipitation Analysis.** Triton X-100 soluble fraction of cauda sperm (50 $\mu$ g protein) was immunoprecipitated with anti-FGL2 and fractionated by SDS-PAGE on a 12% gel followed by immunoblot analyses. Immunoreactive bands were detected by LICOR Odyssey CVX imaging system. Sperm lysate lanes reveal the presence of FGL2 (A-lane 1) and Annexin V (B-lane 3). As shown in figure A-lane 2, FGL2 was recovered in the anti-FGL2 immunoprecipitated (IP) pellet, whereas Annexin V co-precipitated with FGL2 (Figure B-lane 4).

**Acknowledgements:** Supported by NIH grant 5SC3GM125488 (Subir K Nagdas) and GM 103499 (Sub PI: S. Raychoudhury).

**Conflict of Interest:** The author(s) declare(s) that there is no conflict of interest regarding the publication of this article.

## References

- Bedford JM (1975) Maturation, transport, and fate of spermatozoa in the epididymis. In: Greep RO, et al. (Eds.), Handbook of Physiology: Endocrinology, Male Reproductive System, Waverly Press, New York, USA, pp: 303-317.
- Orgebin MC, Danzo BJ, Davies J (1975) Endocrine control of the development and maintenance of sperm fertilizing ability in the epididymis. In: Greep RO, et al. (Eds.), Handbook of Physiology: Endocrinology, Male Reproductive System, Waverly Press, New York, USA, pp: 319-338.
- Robaire B, Hermo L (1988) Efferent ducts, epididymis, and vas deferens: structure, function, and their regulation. In: Knobil E, (Eds.), The physiology of reproduction, Raven Press, New York, USA, pp: 999-1080.
- Turner TT (1995) On the epididymis and its role in the development of the fertile ejaculate. J Androl 16(4): 292-298.
- Hinton BT, Palladino MA (1995) Epididymal epithelium: Its contribution to the formation of a luminal fluid microenvironment. Microsc Res Tech 30(1): 67-81.
- Orgebin CM (1996) Androgens and epididymal function. Pharmacology, biology, and clinical applications of androgens. Wiley-Liss, pp: 27-38.
- Hinton BT, Palladino MA, Rudolph D, Lan ZJ, Labus JC (1996) The role of the epididymis in the protection of spermatozoa. Curr Top Dev Biol 33: 61-102.
- Friend DS, Gilula NB (1972) Variations in tight and gap junctions in mammalian tissues. J Cell Biol 53(3): 758-776.
- Hamilton DW (1975) Structure and function of the epithelium lining the ductuli efferentes, ductus epididymidis, and ductus deferens in the rat. In Greep RO, et al. (Eds.), Handbook of Physiology: Endocrinology, Male Reproductive System, Waverly Press, New York, USA, pp: 259-301.
- Bartles JR (1995) The spermatid plasma membrane comes of age. Trends Cell Biol 5(10): 400-404.
- Kirchhoff C, Pera I, Derr P, Yeung CH, Cooper T (1997) The molecular biology of the sperm surface. Post-testicular membrane remodelling. Adv Exp Med Biol 424: 221-232.
- Jones RC (1999) To store or mature spermatozoa? The primary role of the epididymis. Int J Androl 22(2): 57-67.

13. Robaire B, Viger RS (1995) Regulation of epididymal epithelial cell functions. *Biol Reprod* 52(2): 226-236.
14. Kirchhoff C, Osterhoff C, Pera I, Schroter S (1998) Function of human epididymal proteins in sperm maturation. *Andrologia*, 30(4-5): 225-232.
15. Cornwall GA, Orgebin MC, Hann SR (1992) The CRES gene: a unique testis-regulated gene related to the cystatin family is highly restricted in its expression to the proximal region of the mouse epididymis. *Mol Endocrinol* 6(10): 1653-1664.
16. Glover TD (1961) Disintegrated spermatozoa from the epididymis. *Nature* 190: 185-186.
17. Cooper TG, Hamilton DW (1977) Observations on destruction of spermatozoa in the cauda epididymis and proximal vas deferens of non-seasonal male mammals. *Am J Anat* 149(1): 93-110.
18. Weissenberg R, Yossefi S, Oschry Y, Madgar I, Lewin LM (1994) Investigations of epididymal sperm maturation in the golden hamster. *Int J Androl* 17(5): 256-261.
19. Martan J (1969) Epididymal histochemistry and physiology. *Biol Reprod Suppl* 1: 134-154.
20. Olson GE, Winfery VP, Nagdas SK, Melner MH (2004) Region-specific expression and secretion of the fibrinogen-related protein, fgl2, by epithelial cells of the hamster epididymis and its role in disposal of defective spermatozoa. *J Biol Chem* 279(49): 51266-51274.
21. Pollanen P, Cooper TG (1994) Immunology of the testicular excurrent ducts. *J Reprod Immunol* 26(3): 167-216.
22. Marazzi S, Blum S, Hartmann R, Gundersen D, Schreyer M, et al. (1998) Characterization of human fibroleukin, a fibrinogen-like protein secreted by T lymphocytes. *J Immunol* 161(1): 138-147.
23. Hengartner MO (2000) The biochemistry of apoptosis. *Nature* 407(6805): 770-776.
24. Gorczyca W, Traganos F, Jesionowska H, Darzynkiewicz Z (1993) Presence of DNA strand breaks and increased sensitivity of DNA in situ to denaturation in abnormal human sperm cells: Analogy to apoptosis of somatic cells. *Exp Cell Res* 207(1): 202-205.
25. Baccetti B, Collodel G, Piomboni P (2001) Apoptosis in human ejaculated sperm cells (*Notulae seminologicae* 9). *J Submicrosc Cytol Patho* 28(4): 587-596.
26. Weil M, Jacobson MD, Raff MC (1998) Are caspases involved in the death of cells with a transcriptionally inactive nucleus? Sperm and chicken erythrocytes. *J Cell Sci* 111(pt 18): 2707-2715.
27. Yin Y, Stahl BC, DeWolf WC, Morgentaler A (1998) p53-mediated germ cell quality control in spermatogenesis. *Dev Biol* 204(1): 165-171.
28. Sakkas D, Mariethoz E, John JC (1999) Abnormal sperm parameters in humans are indicative of an abortive apoptotic mechanism linked to the Fas-mediated pathway. *Exp Cell Res* 251(2): 350-355.
29. Roussel JD, Stallcup OT, Austin CR (1967) Selective phagocytosis of spermatozoa in the epididymis of bulls, rabbits, and monkeys. *Fertili Steril* 18(4): 509-516.
30. Smith PD, Bedford JM (1978) Fate of spermatozoa in the male: II. Absence of a specific sperm disposal mechanism in the androgen-deficient hamster and rabbit. *Biol Reprod* 18(5): 791-798.
31. Flickinger CJ (1982) The fate of sperm after vasectomy in the hamster. *Anat Rec* 202(2): 231-239.
32. Glander HJ, Schaller J (1999) Binding of annexin V to plasma membranes of human spermatozoa: a rapid assay for detection of membrane changes after cryostorage. *Mol Hum Reprod* 5(2): 109-115.
33. Muller K, Pomorski T, Muller P, Herrmann A (1999) Stability of transbilayer phospholipid asymmetry in viable ram sperm cells after cryotreatment. *J Cell Sci* 112(pt 1): 11-20.
34. Barroso G, Morshedi M, Oehninger S (2000) Analysis of DNA fragmentation, plasma membrane translocation of phosphatidylserine and oxidative stress in human spermatozoa. *Hum Reprod* 15(6): 1338-1344.
35. Duru NK, Morshedi M, Schuffner A, Oehninger S (2001) Cryopreservation-thawing of fractionated human spermatozoa and plasma membrane translocation of phosphatidylserine. *Fertili Steril* 75(2): 263-268.
36. Ramos L, Wetzels AM (2001) Low rates of DNA fragmentation in selected motile human spermatozoa assessed by the TUNEL assay. *Hum Reprod* 16(8): 1703-1707.
37. Tyurina YY, Shvedova AA, Kawai K, Tyurin VA, Kommineni C, et al. (2000) Phospholipid signaling in apoptosis: peroxidation and externalization of phosphatidylserine. *Toxicology* 148(2-3): 93-101.
38. Balasubramanian K, Bevers EM, Willems GM, Schroit AJ (2001) Binding of annexin V to membrane products of

- lipid peroxidation. *Biochemistry* 40(30): 8672-8676.
39. Zieseniss S, Zahler S, Muller I, Hermetter A, Engelmann B (2001) Modified phosphatidylethanolamine as the active component of oxidized low density lipoprotein promoting platelet prothrombinase activity. *J Bio Chem* 276(23): 19828-19835.
  40. Poulos A, Bennett AD, White IG (1973) The phospholipid-bound fatty acids and aldehydes of mammalian spermatozoa. *Comp Biochem Physiol* 46(3): 541-549.
  41. Jones R, Mann T, Sherins R (1979) Peroxidative breakdown of phospholipids in human spermatozoa, spermicidal properties of fatty acid peroxides, an protective action of seminal plasma. *Fertil Steril* 31(5): 531-537.
  42. Nolan JP, Hammerstedt RH (1997) Regulation of membrane stability and the acrosome reaction in mammalian sperm. *FASEB J* 11(8): 670-682.
  43. Ladha S (1998) Lipid heterogeneity and membrane fluidity in a highly polarized cell, the mammalian spermatozoon. *J Membr Bio* 165(1): 1-10.
  44. Jones R, Mann T (1977) Damage to ram spermatozoa by peroxidation of endogenous phospholipids. *J Reprod and Fertil* 50(2): 261-268.
  45. Alvarez E, Storey BT (1982) Spontaneous lipid peroxidation in rabbit epididymal spermatozoa: its effect on sperm motility. *Biol Reprod* 27(5): 1102-1108.
  46. Baarends WM, Roest HP, Grootegoed JA (1999) The ubiquitin system in gametogenesis. *Mol Cell Endocrinol* 151(1-2): 5-16.
  47. Sutovsky P, Moreno R, Santos JR, Dominko T, Thompson WE, et al. (2001a) A putative, ubiquitin-dependent mechanism for the recognition and elimination of defective spermatozoa in the mammalian epididymis. *J Cell Sci* 114(pt 9): 1665-1675.
  48. Sutovsky P, Terada Y, Schatten G (2001b) Ubiquitin-based sperm assay for the diagnosis of male factor infertility. *Hum Reprod* 16(2): 250-258.
  49. Cooper TG, Yeung CH, Jones R, Orgebin MC, Robaire B (2002) Rebuttal of a role for the epididymis in sperm quality control by phagocytosis of defective sperm. *J Cell Sci* 115(pt 1): 5-7.
  50. Amours O, Frenette G, Bordeleau LJ, Allard N, Leclerc P, et al. (2012) Epididymosomes transfer epididymal sperm binding protein 1 (ELSPBP1) to dead spermatozoa during epididymal transit in bovine. *Biol Reprod* 87(4): 1-11.
  51. NagDas SK, Winfrey VP, Olson GE (2000) Identification of a hamster epididymal region-specific secretory glycoprotein that binds nonviable spermatozoa. *Biol Reprod* 63(5): 1428-1436.
  52. Doolittle RF (2001) A detailed consideration of a principal domain of vertebrate fibrinogen and its relatives. *Protein Sci* 1(12): 1563-1577.
  53. Koyama T, Hall LR, Haser WG, Tonegawa S, Saito H (1987) Structure of a cytotoxic T-lymphocyte-specific gene shows a strong homology to fibrinogen b and g chains. *Proc Natl Acad U S A* 84(6): 1609-1613.
  54. Ruegg C, Pytela R (1995) Sequence of a human transcript expressed in T-lymphocytes and encoding a fibrinogen-like protein. *Gene* 160(2): 257-262.
  55. Levy GA, Liu M, Ding J, Yuwaraj S, Leibowitz J (2000) Molecular and functional analysis of the human prothrombinase gene (HFGL2) and its role in viral hepatitis. *Am J Pathol* 156(4): 1217-1225.
  56. Nagdas SK, Winfrey VP, Olson GE (2016) Two Fibrinogen-Like Proteins, FGL1 and FGL2 are Disulfide-Linked Subunits of Oligomers That Specifically Bind Nonviable Spermatozoa. *Int J Biochem Cell Biol* 80: 163-172.
  57. Yamamoto T, Gotoh M, Sasaki H, Terada M, Kitajima M, et al. (1993) Molecular cloning and initial characterization of a novel fibrinogen-related gene- HFREP-1. *Biochem Biophys Res Commun* 193(2): 681-687.
  58. Hara H, Uchida S, Yoshimura H, Aoki M, Toyoda Y, et al. (2000) Isolation and characterization of a novel liver-specific gene, hepassocin, upregulated during liver regeneration. *Biochim Biophys Acta* 1492(1): 31-44.
  59. Yan J, Ying H, Gu F, He J, Li YL, et al. (2002) Cloning and characterization of a mouse liver-specific gene mfrep-1, up-regulated in liver regeneration. *Cell Res* 12(5-6): 353-361.
  60. Li CY, Cao CZ, Xu WX, Cao MM, Yang F, et al. (2010) Recombinant human hepassocin stimulates proliferation of hepatocytes in vivo and improves survival in rats with fulminant hepatic failure. *Gut* 59(6): 817-826.
  61. Demchev V, Malana G, Vangala D, Stoll J, Desai A, et al. (2013) Targeted deletion of fibrinogen like protein 1 reveals a novel role in energy substrate utilization. *PLoS One* 8(3): e58084.
  62. Hashemi HN, Desai A, Demchev V, Bronson RT, Hornick JL, et al. (2015) Targeted disruption of fibrinogen

- like protein-1 accelerates hepatocellular carcinoma development. *Biochem Biophys Res Commun* 465(2): 167-173.
63. Nagdas SK, Wallace S, Eaford D, Baker R, Carr K, et al. (2020) Fibrinogen-related protein, FGL2, of hamster cauda epididymal fluid: Purification, kinetic analysis of its prothrombinase activity, and its role in segregation of nonviable spermatozoa. *Mol Reprod Dev* 87(12): 1206-1218.
  64. NagDas SK, Winfrey VP, Olson GE (1996a) Proacrosin-acrosomal matrix binding interactions in ejaculated bovine spermatozoa. *Biol Reprod* 54(1): 111-121.
  65. Laemmli UK (1970) Cleavage of structural proteins during the assembly of the head of bacteriophage T4. *Nature* 227(5259): 680-685.
  66. Fairbanks G, Steck TL, Wallach DFH (1971) Electrophoretic analysis of the major polypeptides of the human erythrocyte membrane. *Biochemistry* 10(13): 2606-2617.
  67. Towbin H, Staehelin T, Gordon J (1979) Electrophoretic transfer of proteins from polyacrylamide gels to nitrocellulose sheets: Procedure and some applications. *Proc Natl Acad Sci* 76(9): 4350-4354.
  68. Bradford MM (1976) A rapid and sensitive method for the quantitation of microgram quantities of protein utilizing the principle of protein-dye binding. *Anal Biochem* 72: 248-254.
  69. Olson GE, Winfrey VP (1985) Substructure of a cytoskeletal complex associated with the hamster sperm acrosome. *J Ultrastruct Res* 92(3): 167-179.
  70. NagDas SK, Winfrey VP, Olson GE (1996b) Identification of hydrolase binding activities of the acrosomal matrix of hamster spermatozoa. *Biol Reprod* 55(6): 1405-1414.
  71. Parr RL, Fung L, Reneker J, Mason NM, Leibowitz J, et al. (1995) Association of mouse fibrinogen-like protein with murine hepatitis virus-induced prothrombinase activity. *J Virol* 69(8): 5033-5038.
  72. Nielsen H, Engelbrecht J, Brunak S, Heijne GV (1997) Identification of prokaryotic and eukaryotic signal peptides and prediction of their cleavage sites. *Protein Eng* 10(1): 1-6.
  73. Yuwaraj S, Ding JW, Liu M, Marsden PA, Levy GA (2001) Genomic characterization, localization, and functional expression of FGL2, the human gene encoding fibroleukin: A novel human procoagulant. *Genomics* 71(13): 330-338.
  74. Marsden PA, Ning Q, Fung LS, Luo X, Chen Y, et al. (2003) The fgl2/fibroleukin prothrombinase contributes to immunologically mediated thrombosis in experimental and human viral hepatitis. *J Clin Invest* 112(1): 58-66.
  75. Rawlings ND, Barrett AJ (1994) Families of serine peptidases. *Methods Enzymol* 244: 19-61.
  76. Barrett AJ, Rawlings ND (1995) Families and clans of serine peptidases. *Arch Biochem Biophys* 318(2): 247-250.
  77. Dahlback B (2000) Blood coagulation. *Lancet* 355(9215): 1627-1632.
  78. Shalev I, Liu H, Kosciak C, Bartczak A, Javadi M, et al. (2008) Targeted deletion of fgl2 leads to impaired regulatory T cell activity and development of autoimmune glomerulonephritis. *J Immunol* 180(1): 249-260.
  79. Yuan K, Feng Y, Wang H, Zhao L, Wang W, et al. (2020) FGL2 is positively correlated with enhanced antitumor responses mediated by T cells in lung adenocarcinoma. *PeerJ* 8: e8654.
  80. Yu J, Li J, Shen J, Du F, Wu X, et al. (2021) The role of Fibrinogen-like proteins in Cancer. *Int J of Biol Sci* 17(4): 1079-1087.
  81. Zeng M, Li Q, Chen J, Huang W, Liu J, et al. (2022) The Fgl2 interaction with Tyrobp promotes the proliferation of cutaneous squamous cell carcinoma by regulating ERK-dependent autophagy. *Int J Med Sci* 19(1): 195-204.
  82. Elesawy FM, Hafeez NA, Abdelsalam OH, Akl EM (2020) Soluble Fibrinogen-like protein 2 plays a role in varicocele induced male infertility. *Andrologia* 52(6): e13626.
  83. Carrera A, Gerton GL, Moss SB (1994) The major fibrous sheath polypeptide of mouse sperm: structural and functional similarities to the A-kinase anchoring proteins. *Dev Biol* 165(1): 272-284.
  84. Fulcher KD, Mori C, Welch JE, Brien DA, Klapper DG, et al. (1995) Characterization of Fsc1 cDNA for a mouse sperm fibrous sheath component. *Biol Reprod* 52(1): 41-49.
  85. Carrera A, Moos J, Ning XP, Gerton GL, Kopf GS, (1996) Regulation of protein tyrosine phosphorylation in human sperm by a calcium/calmodulin-dependent mechanism: identification of A kinase anchor proteins as major substrates for tyrosine phosphorylation. *Dev Biol* 180(1): 284-296.
  86. Turner RM, Johnson LR, Ladewig L, Gerton GL, Moss SB (1998) An X-linked gene encodes a major human sperm



- fibrous sheath protein, hAKAP82. Genomic organization, protein kinase A-RII binding, and distribution of the precursor in the sperm tail. *J Biol Chem* 273(48): 32135-32141.
87. Colledge M, Scott JD (1999) AKAPs: from structure to function. *Trends Cell Biol* 9(6): 216-221.
  88. Eddy EM, Toshimori K, Brien DA (2003) Fibrous sheath of mammalian spermatozoa. *Microsc Res Tech* 61(1): 103-115.
  89. Nixon B, Bernstein IR, Cafe SL, Delehedde M, Sergeant N, et al. (2019) A Kinase Anchor Protein 4 Is Vulnerable to Oxidative Adduction in Male Germ Cells. *Front Cell Dev Biol* 7: 319.
  90. Edwards AS, Scott JD (2000) A-kinase anchoring proteins: protein kinase A and beyond. *Curr Opin Cell Biol* 12(2): 217-221.
  91. Brown PR, Miki K, Harper DB, Eddy EM (2003) A-kinase anchoring protein 4 binding proteins in the fibrous sheath of the sperm flagellum. *Biol Reprod* 68(6): 2241-2248.
  92. Miki K, Willis WD, Brown PR, Goulding EH, Fulcher KD, et al. (2002) Targeted disruption of the Akap4 gene causes defects in sperm flagellum and motility. *Dev Biol* 248(2): 331-342.
  93. Mandal A, Hansen S, Wolkowicz MJ, Klotz K, Shetty J, et al. (1999) FSP95, a testis-specific 95-kilodalton fibrous sheath antigen that undergoes tyrosine phosphorylation in capacitated human spermatozoa. *Biol Reprod* 61(5): 1184-1197.
  94. Vijayaraghavan S, Liberty GA, Mohan J, Winfrey VP, Olson GE, et al. (1999) Isolation and molecular characterization of AKAP110, a novel, sperm-specific protein kinase A-anchoring protein. *Mol Endocrinol* 13(5): 705-717.
  95. Zhang G, Li D, Tu C, Meng L, Tan Y, et al. (2021) Loss-of-function missense variant of AKAP4 induced male infertility through reduced interaction with QRICH2 during sperm flagella development. *Hum Mol Genet* 31(2): 219-231.
  96. Ursini F, Heim S, Kiess M, Maiorino M, Roveri A, et al. (1999) Dual function of the selenoprotein PHGPx during sperm maturation. *Science* 285(5432): 1393-1396.
  97. Flohe L (2007) Selenium in mammalian spermiogenesis. *Biol Chem* 388(10): 987-995.
  98. Imai H, Nakagawa Y (2003) Biological significance of phospholipid hydroperoxide glutathione peroxidase (PHGPx, GPx4) in mammalian cells. *Free Rad Biol Med* 34(2): 145-169.
  99. Foresta C, Flohe L, Garolla L, Roveri A, Ursini F, et al. (2002) Male fertility is linked to the selenoprotein phospholipid hydroperoxide glutathione peroxidase. *Biol Reprod* 67(3): 967-971.
  100. Alvarez JG, Touchstone JC, Blasco L, Storey BT (1987) Spontaneous lipid peroxidation and production of hydrogen peroxide and superoxide in human spermatozoa. Superoxide dismutase as major enzyme protectant against oxygen toxicity. *J Androl* 8(5): 338-348.
  101. Rao B, Soufir JC, Martin M, David G (1989) Lipid peroxidation in human spermatozoa as related to midpiece abnormalities and motility. *Gamete Res* 24(2): 127-134.
  102. Armstrong J, Rajasekaran M, Chamulitrat W, Gatti P, Hellstrom W, et al. (1999) Characterization of reactive oxygen species induced effects on human spermatozoa movement and energy metabolism. *Free Rad Biol Med* 26(7-8): 869-880.
  103. Imai H, Suzuki K, Ishizaka K, Ichinose S, Oshima H, et al. (2001) Failure of the expression of phospholipid hydroperoxide glutathione peroxidase in the spermatozoa of human infertile males. *Biol Reprod* 64(2): 674-683.
  104. He B, Guo H, Gong Y, Zhao R (2017) Lipopolysaccharide-induced mitochondrial dysfunction in boar sperm is mediated by activation of oxidative phosphorylation. *Theriogenology* 87: 1-8.
  105. Ferrandi B, Consiglio AL, Carnevali A, Porcelli F (1989) Cytochrome oxidase and lactate dehydrogenase activities in peroxidized rabbit epididymal spermatozoa. *Andrologia* 21(3): 215-222.
  106. Henson PM, Bratton DL, Fadok VA (2001) The phosphatidylserine receptor: a crucial molecular switch. *Nat Rev Mol Cell Biol* 2(8): 627-633.
  107. Fadok VA, Bratton DL, Rose DM, Pearson A, Ezekewitz RA, et al. (2000) A receptor for phosphatidylserine-specific clearance of apoptotic cells. *Nature* 405(6782): 85-90.
  108. Ladha S, James PS, Clark DC, Howes EA, Jones R (1997) Lateral mobility of plasma membrane lipids in bull spermatozoa: heterogeneity between surface domains and rigidification following cell death. *J Cell Sci* 110(pt 9): 1041-1050.

109. Aitken RJ, Harkiss D, Buckingham DW (1993) Analysis of lipid peroxidation mechanisms in human spermatozoa. *Mole Reprod Dev* 35(3): 302-315.
110. Storey BT (1997) Biochemistry of the induction and prevention of lipoperoxidative damage in human spermatozoa. *Mol Hum Reprod* 3(3): 203-213.
111. Aitken R J, Vernet P (1998) Maturation of redox regulatory mechanisms in the epididymis. *J Reprod Fertil. Supplem* 53: 109-118.
112. Chan CWY, Chan MWC, Liu M, Fung L, Cole EH, (2002) Kinetic analysis of a unique direct prothrombinase, fgl2, and identification of a serine residue critical for the prothrombinase activity. *J Immunol* 168(10): 5170-5177.
113. Chan CWY, Kay LS, Khadaroo RG, Chan MWC, Lakatoo S, et al. (2003) Soluble fibrinogen-like protein 2/fibroleukin exhibits immunosuppressive properties: Suppressing T cell proliferation and inhibiting maturation of bone marrow-derived dendritic cells. *J Immunol* 170(8): 4036-4044.
114. Dahl MR, Thoenes W, Matsushita M, Fujita T, Willis AC, et al. (2001) MASP-3 and its association with distinct complexes of the mammalian-binding lectin complement activation pathway. *Immunity* 15(1): 127-135.
115. Fujita T (2002) Evolution of the lectin-complement pathway and its role in innate immunity. *Nat Rev Immunol* 2(5): 346-353.
116. Holmskov U, Thiel S, Jensenius JC (2003) Collections and ficolins: Humoral lectins of the innate immune defense. *Annu Rev Immunol* 21: 547-578.

